



Magnetic relaxation in V_{15} cluster: Direct spin-phonon transitions

Alex Tarantul, Boris Tsukerblat*

Department of Chemistry, Ben-Gurion University of the Negev, P.O. Box 653, 84105 Beer-Sheva, Israel

ARTICLE INFO

Article history:

Available online 18 August 2010

Dedicated to Professor Achim Müller-to highlight his exceptional achievements.

Keywords:

Molecular magnetism
Cluster V_{15}
Exchange interaction
Antisymmetric exchange
Spin-phonon relaxation
Coherence

ABSTRACT

In this article we propose a model of spin-vibronic relaxation in $K_6[V^{IV}_{15}As_6O_{42}(H_2O)] \cdot 8H_2O$, the so called V_{15} cluster exhibiting the unique layered structure. The work is motivated by the recent observation of the Rabi oscillation [1] in this system and aimed to elucidate the nature of the relaxation processes. The model assumes that the spin-phonon coupling arises as a result of modulation of the isotropic and antisymmetric (Dzyaloshinsky–Moriya) exchange interactions in the central triangular layer of vanadium ions by the acoustic lattice vibrations. Within the pseudo-angular momentum representation the selection rules for the direct (one-phonon) transitions between Zeeman levels are derived and a special role of the antisymmetric exchange is underlined. The relaxation times related to one-phonon transitions in different ranges of the field are estimated within the Debye model for the lattice vibrations.

© 2010 Elsevier B.V. All rights reserved.

1. Introduction

During last two decades the fundamental discoveries of Achim Müller in polyoxometalate chemistry led to unprecedented progress in this field including fascinating applications to single molecule magnetism, biophysics and nanomaterials science. Design and study of new nanoscopic objects possessing both beauty and intriguing properties facilitated a new development of fundamental issues of nanophysics (see a comprehensive book [2]). About 20 years ago one of us (B.Ts.) started to collaborate with Achim Müller on magnetic mixed valence polyoxometalates [3,4]. Last years this fruitful and pleasant collaboration got a new impact under the auspices of the German-Israel Science foundation [1,5–13] and was focused mainly on the study of famous V_{15} cluster synthesized in Bielefeld. In this article written in honor of Achim Müller we propose a model of spin-phonon relaxation and evaluate the probability of one-phonon processes in the low lying magnetic sublevels in V_{15} . The work is motivated by the recent observation of the Rabi oscillations in this system [1] and aimed to elucidate the role of spin-phonon relaxation as a possible mechanism of decoherence.

The unique cluster anion present in $K_6[V^{IV}_{15}As_6O_{42}(H_2O)] \cdot 8H_2O$ containing fifteen V^{IV} ions ($S_i = 1/2$) and exhibiting the unique layered structure was discovered two decades ago [14] and pioneer studies of this system dates back to this period [14–17]. The synthesis of this fascinating spin frustrated cluster opened a new trend in molecular magnetism closely related to the promising field of single molecule magnets that is expected to give a revolutionary

impact on the design of new memory storage devices of molecular size and quantum computing [2].

The molecular cluster V_{15} has a distinct layered quasi-spherical structure [14,15]. Fifteen V^{IV} ions ($S_i = 1/2$) are placed in a large central triangle sandwiched by two distorted hexagons possessing overall D_3 symmetry (Fig. 1).

Studies of the adiabatic magnetization and quantum dynamics show that the V_{15} cluster exhibits the hysteresis loop of magnetization [18–23] and can be referred to as a mesoscopic system on the border line between the classical and quantum world. The studies of the static magnetic susceptibility [16,17], energy pattern [24–32], *ab initio* electronic structure calculations [33–37] and inelastic neutron scattering (INS) [38,39] showed that the low lying part of the energy spectrum is well isolated from the remaining spin levels and can be understood as a result of interaction between three moieties consisting of five strongly coupled spins giving rise to spin $S_i = 1/2$ of each moiety. The studies of V_{15} cluster are reviewed in Ref. [40].

A novel route to employ the properties of molecular magnets is a spin-based implementation of quantum information processing that is expected to provide a development in the problem of quantum computing [1,41–53]. The key question formulated in Ref. [41] is: “will decoherence times in molecular magnets permit quantum information processing?” First prediction of the coherent states in V_{15} has been made in Ref. [54] where it was explicitly stated: “...quantum coherence in a V_{15} molecule is not suppressed and, in principle, can be detected experimentally.” In fact, recent observation and interpretation of the Rabi oscillation in V_{15} have been reported in Ref. [1]. In Ref. [54] different mechanisms of decoherence have been discussed and in particular a general estimation

* Corresponding author. Tel.: +972 8 647 93 61; fax: +972 8 647 29 43.
E-mail address: tsuker@bgu.ac.il (B. Tsukerblat).

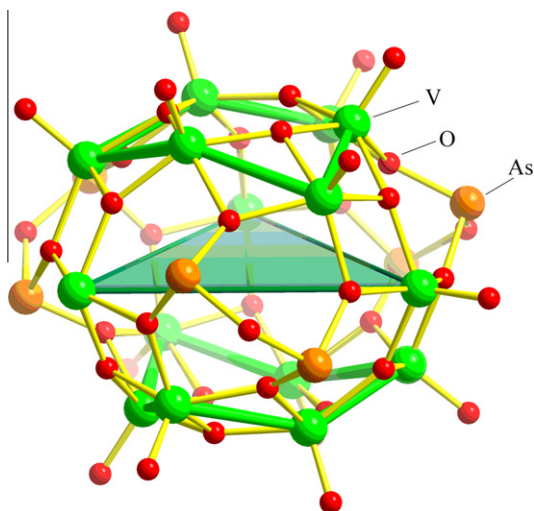


Fig. 1. Ball-and-stick representation the cluster anion $[V^{IV}_{15}As_6O_{42}(H_2O)]^{6-}$ emphasizing the V_3 triangle (the central water molecule is not indicated) [14].

of the order of magnitude of spin-phonon relaxation times has been made. In this article we propose a microscopic approach to the evaluation of the rates of the direct (one-phonon) spin lattice relaxation based on the accurate consideration of the spin states and Zeeman levels of V_{15} , and a simple Debye model for the lattice vibrations. In the subsequent studies this model will be extended and employed for a more general studies of phonon-assisted processes in molecular magnets, including two-phonon and Orbach-type transitions.

2. Triangle model for V_{15} cluster

The model of spin triangle for the low lying spin excitations suggested in Refs. [16,20] includes isotropic Heisenberg–Dirac–Van Vleck (HDVV) exchange interaction and antisymmetric (AS) exchange proposed by Dzyaloshinsky [55] and Moriya [56] as an origin of spin canting in magnetic materials (see Refs. [18–20]). The last interaction was shown [57,58] to be especially important for the spin frustrated system possessing triangular structure. A model of an effective spin triangle [16,17] of vanadium ions ($S = 1/2$) that provides an adequate description of the whole system at low temperatures when the spin of hexagons are paired due to relatively strong antiferromagnetic interactions while the coupling inside the triangle is relatively small. This vanadium triangle that is a central magnetic layer in the V_{15} structure is shaded in Fig. 1. Three spins of the central triangle are coupled through the antiferromagnetic isotropic exchange. The full Hamiltonian of the system looks as:

$$H \equiv H_0 + H_{AS} = 2J(\mathbf{S}_1\mathbf{S}_2 + \mathbf{S}_2\mathbf{S}_3 + \mathbf{S}_3\mathbf{S}_1) + \sum_{ij} \mathbf{D}_{ij} [\mathbf{S}_i \times \mathbf{S}_j] \quad (1)$$

The eigen-values of the Hamiltonian H_0 with the antiferromagnetic ($J > 0$) coupling includes two levels, namely “accidentally” degenerate spin doublets (ground level) and excited spin quadruplet separated by the gap $3J$. According to the overall point symmetry D_3 the vector constants \mathbf{D}_{ij} ($ij = 12, 23, 31$ numerate the sides) of the AS exchange have, in general, three independent components, namely, along and perpendicular to the side (in plane of the triangle) and perpendicular to the plane component whose absolute values are respectively D_l , D_r and D_n . Consequently the Hamiltonian H_{AS} can be divided into two parts, $H_{AS}(\parallel)$ (“normal”) and $H_{AS}(\perp)$ (“in-plane”) which are defined as:

$$H_{AS}(\parallel) = D_n([\mathbf{S}_1 \times \mathbf{S}_2]_Z + [\mathbf{S}_2 \times \mathbf{S}_3]_Z + [\mathbf{S}_3 \times \mathbf{S}_1]_Z) \quad (2)$$

$$H_{AS}(\perp) = D_l \left([\mathbf{S}_1 \times \mathbf{S}_2]_X - \frac{1}{2} [\mathbf{S}_2 \times \mathbf{S}_3]_X + \frac{\sqrt{3}}{2} [\mathbf{S}_2 \times \mathbf{S}_3]_Y - \frac{1}{2} [\mathbf{S}_3 \times \mathbf{S}_1]_X - \frac{\sqrt{3}}{2} [\mathbf{S}_3 \times \mathbf{S}_1]_Y \right) + D_r \left([\mathbf{S}_1 \times \mathbf{S}_2]_Y - \frac{\sqrt{3}}{2} [\mathbf{S}_2 \times \mathbf{S}_3]_X - \frac{1}{2} [\mathbf{S}_2 \times \mathbf{S}_3]_Y + \frac{\sqrt{3}}{2} [\mathbf{S}_3 \times \mathbf{S}_1]_X - \frac{1}{2} [\mathbf{S}_3 \times \mathbf{S}_1]_Y \right) \quad (3)$$

where the axes X and Y of the global coordinates system are directed as shown in Fig. 2 while the axis Z is perpendicular to the plane (right-hand coordinate system). These two parts of the AS exchange are explicitly separated as they play quite different physical roles. The normal part of AS exchange splits the ground doublets (the splitting being $\sqrt{3}D_n$) and gives rise to a strong (first order) magnetic anisotropy while the in-plane part is responsible for the doublet-quadruplet mixing. This mixing leads to a second order zero-field splitting of the $S = 3/2$ level (that is $(D_l^2 + D_r^2)/8J$). It was shown [5] that D_l and D_r are combined into an effective parameter $D_{\perp} = \sqrt{D_l^2 + D_r^2}$ so the model is fully specified by the three parameters J , D_n and D_{\perp} . The parameter J is found to be about 0.85 cm^{-1} [4] and recent estimation based on the low temperature magnetization data [19] provides the following AS exchange constants: $D_{\perp} = 0.24 \text{ cm}^{-1}$, $D_n = 0.08 \text{ cm}^{-1}$ [57,58].

3. Spin-phonon interaction

The interaction of spins with the lattice vibrations (heat reservoir) arises from the modulation of the isotropic and AS exchange interactions by the molecular displacements X_i, Y_i, Z_i ($i = 1, 2, 3$ enumerates the ions) in course of the lattice vibrations [59–61]. It is convenient to deal with the symmetry adapted coordinates Q_{α} (α enumerates the vibrational mode) of the equilateral triangular unit: full symmetric A_1 ($Q_{A_1} \equiv Q_A$) and double degenerate E type ($Q_{E_x} \equiv Q_x, Q_{E_y} \equiv Q_y$). These normal coordinates can be expressed in terms of the Cartesian displacements X_i, Y_i, Z_i of the constituent

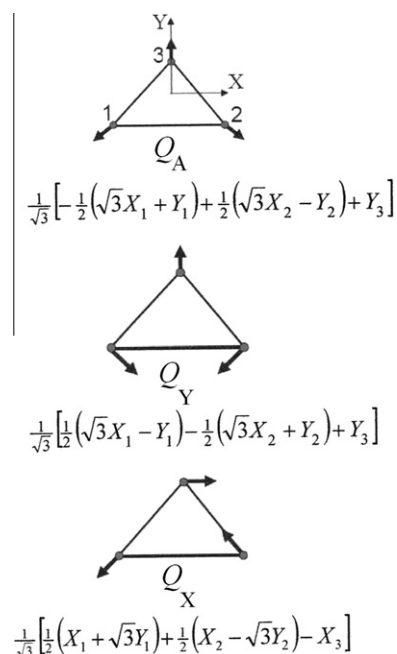


Fig. 2. Vibrational coordinates of a symmetric triangular unit exchange.

ions as shown in Fig. 2. Within this mechanism of spin-phonon (vibronic) interaction the exchange parameters are assumed to be the functions of the metal-metal distances R_{ij} so that the linear (with respect to the displacements) terms of the vibronic Hamiltonian H_{ev} can be represented as a sum of two contributions $H_{ev} = H'_{ev} + H''_{ev}$, where H'_{ev} and H''_{ev} are the contributions of the isotropic and AS parts of the exchange Hamiltonian respectively. They can be written as:

$$H'_{ev} = \sum_{\alpha=A,X,Y} \left(\frac{\partial H_0}{\partial Q_\alpha} \right)_{Q_\alpha=0} Q_\alpha, \quad (4)$$

$$H''_{ev} = \sum_{\alpha=A,X,Y} \left(\frac{\partial H_{AS}}{\partial Q_\alpha} \right)_{Q_\alpha=0} Q_\alpha. \quad (5)$$

After substitution of the corresponding parts of the exchange Hamiltonian one obtains the following expressions for the spin-phonon coupling operators:

$$H'_{ev} = \sum_{ij} \sum_{\alpha=A,X,Y} 2\mathbf{s}_i \mathbf{s}_j \left(\frac{\partial J_{ij}(R_{ij})}{\partial R_{ij}} \right)_{\Delta R_{ij}=0} \cdot \frac{\partial R_{ij}}{\partial Q_\alpha} Q_\alpha \quad (6)$$

$$H''_{ev} = \sum_{ij} \sum_{\alpha=A,X,Y} \mathbf{s}_i \times \mathbf{s}_j \left(\frac{\partial \mathbf{D}_{ij}(R_{ij})}{\partial R_{ij}} \right)_{\Delta R_{ij}=0} \cdot \frac{\partial R_{ij}}{\partial Q_\alpha} Q_\alpha \quad (7)$$

where R_{ij} are the instant metal-metal distances in course of the vibrations while $\Delta R_{ij} = 0$ corresponds to the equilibrium trigonal configuration and symmetric exchange network with the sides R_0 . Modulation of the isotropic exchange can be described by the parameter λ which is defined as $\lambda \equiv \sqrt{6}(\partial J_{ij}(R_{ij})/\partial R_{ij})$. For each side of the triangle there is also a vector coupling parameter which is related to the AS exchange and defined as $\beta_{ij} = (\partial \mathbf{D}_{ij}(R_{ij})/\partial R_{ij})_0$. Due to the trigonal symmetry of the system the absolute values of these three vector parameters have the same value β for each side of the triangle. One can also define three components of β_{ij} , namely, normal part $\beta_n = \beta_{ijn}$ and two perpendicular contributions $\beta_t = \beta_{ijt}$ and $\beta_l = \beta_{ijl}$ where the symbols l and t have the same meaning as in the definition of the AS exchange Hamiltonian. One can also define a combined vibronic parameter $\beta_\perp = \sqrt{\beta_t^2 + \beta_l^2}$ that appears in the final results. Eq. (3) contains contributions related to the isotropic and AS exchange interactions to the overall vibronic coupling. After calculation of the derivatives $\partial R_{ij}/\partial Q_\alpha$ (using the relations between the Cartesian displacements X_i, Y_i, Z_i and normal coordinates Q_α , Fig. 2) one arrives at the following form of the spin-vibronic Hamiltonian:

$$H'_{ev} = \sum_{\Gamma\gamma} \lambda \hat{V}_{\Gamma\gamma} Q_{\Gamma\gamma} \quad (8)$$

$$H''_{ev} = \sum_{\Gamma\gamma} \beta \hat{W}_{\Gamma\gamma} Q_{\Gamma\gamma}$$

$$H_{ev} = \sum_{\Gamma\gamma} \hat{G}_{\Gamma\gamma} Q_{\Gamma\gamma}, \quad \hat{G}_{\Gamma\gamma} = \lambda \hat{V}_{\Gamma\gamma} + \beta \hat{W}_{\Gamma\gamma}.$$

Here $\Gamma\gamma = A_1, E_x, E_y$ label the irreducible representations and basis functions of the \mathbf{D}_3 symmetry group and the operators $\hat{V}_{\Gamma\gamma}$ and $\hat{W}_{\Gamma\gamma}$ are expressed in terms of the scalar and vector products of spin operators (Appendix I). The evaluation of the vibronic matrices is performed with the aid of the irreducible tensor operators approach [2,60–64].

The vibronic term arising from the modulation of the AS exchange (H''_{ev}) can be divided into two parts ($H''_{ev} = H''_{ev}(\parallel) + H''_{ev}(\perp)$), namely, the part arising from the modulation of $H_{AS}(\parallel)$ and that emerging from the modulation of $H_{AS}(\perp)$. These two parts are denoted as $H''_{ev}(\parallel)$ and $H''_{ev}(\perp)$ respectively:

$$H''_{ev}(\parallel) = \sum_{\alpha=A,X,Y} \left(\frac{\partial H_{AS}(\parallel)}{\partial Q_\alpha} \right)_{Q_\alpha=0} \cdot Q_\alpha, \quad (9)$$

$$H''_{ev}(\perp) = \sum_{\alpha=A,X,Y} \left(\frac{\partial H_{AS}(\perp)}{\partial Q_\alpha} \right)_{Q_\alpha=0} \cdot Q_\alpha.$$

In order to include the interaction of spins with the acoustic lattice vibrations, the symmetry adapted molecular displacement should be expanded into series of the longitudinal (l) and transverse (t) lattice vibrational modes $q_{\kappa\nu}$ specified by the wave vector κ and polarization $\nu = l, t$ as suggested in ref. [65]:

$$Q_{\Gamma\gamma} = \sum_{\kappa\nu} \left(\frac{\hbar}{M\omega_{\kappa\nu}} \right)^{1/2} a_{\kappa\nu}(\Gamma\gamma) q_{\kappa\nu}, \quad \nu = l, t \quad (10)$$

In Eq. (10) $q_{\kappa\nu}$ are the dimensionless normal coordinates of the lattice, M is a mass of crystal and $a_{\kappa\nu}(\Gamma\gamma)$ are the so called Van Vleck coefficients [65] introduced in his underlying theory of paramagnetic relaxation; their exact expressions for a triangular molecule are given in Appendix II. The final expression for the spin-phonon interaction is the following:

$$H_{ev} = \sum_{\Gamma\gamma} \hat{G}_{\Gamma\gamma} \sum_{\kappa\nu} \left(\frac{\hbar}{M\omega_{\kappa\nu}} \right)^{1/2} a_{\kappa\nu}(\Gamma\gamma) q_{\kappa\nu} \quad (11)$$

It should be noted that the spin-phonon Hamiltonian in Eq. (11), is adapted to the triangle model for V_{15} . In fact, by definition the matrices $\hat{G}_{\Gamma\gamma}$ in this Hamiltonian act within the set of eight spin functions (two $S = 1/2$ doublets and quadruplet $S = 3/2$) of the vanadium triangle.

4. One-phonon spin-lattice relaxation

Let us consider the case of two non-degenerate electronic states $|I\rangle$ and $|F\rangle$ separated by the energy gap $\Delta E = E_I - E_F > 0$ and a transition $|I\rangle \rightarrow |F\rangle$ accompanied by the release of a phonon with the energy $\hbar\omega_{\kappa\nu} = \Delta E$. According to the perturbation theory the probability of this transition is the following:

$$w_{\kappa\nu} = \frac{2\pi}{\hbar} \left(\sum_{\Gamma\gamma} \left(\frac{\hbar}{M\omega_{\kappa\nu}} \right) a_{\kappa\nu}^2(\Gamma\gamma) \left| \langle F | \hat{G}_{\Gamma\gamma} | I \rangle \right|^2 \cdot |\langle n_{\kappa\nu} | q_{\kappa\nu} | n_{\kappa\nu} + 1 \rangle|^2 \right) \cdot \delta(\hbar\omega_{\kappa\nu} - \Delta E), \quad (12)$$

where $\delta(x)$ is the Dirac δ -function. After summation over the vibrational modes (including thermal averaging) one arrives at the following expression:

$$w_{I \rightarrow F} = \frac{1}{\pi \hbar \rho} \cdot \frac{\omega_0}{1 - \exp(-\hbar\omega_0/kT)} \cdot \sum_{\Gamma\gamma} \left(\frac{2}{v_l^3} \langle a_l^2(\Gamma\gamma) \rangle + \frac{4}{v_t^3} \langle a_t^2(\Gamma\gamma) \rangle \right) \left| \langle F | \hat{G}_{\Gamma\gamma} | I \rangle \right|^2, \quad (13)$$

where $\hbar\omega_0 = \Delta E$ is the resonance phonon frequency and ρ is the crystal density. Within the Debye model for the lattice vibrations the averaged (over all directions of the phonon propagation vector but with the fixed specified frequency ω) squared Van Vleck coefficients are given in Appendix II. Substitution of these equations into Eq. (13) leads the following result

$$w_{I \rightarrow F} = \frac{R_0^2}{\pi \hbar \rho} \frac{L_{IF}}{1 - \exp(-\Delta E/kT)} \left(\frac{\Delta E}{\hbar} \right)^3, \quad (14)$$

$$L_{IF} = \left| \langle F | \hat{G}_A | I \rangle \right|^2 \left(\frac{1}{15 v_t^5} + \frac{4}{15 v_l^5} \right) + \left| \langle F | \hat{G}_x | I \rangle \right|^2 \left(\frac{1}{5 v_t^5} + \frac{2}{15 v_l^5} \right) + \left| \langle F | \hat{G}_y | I \rangle \right|^2 \left(\frac{1}{5 v_t^5} + \frac{2}{15 v_l^5} \right) \quad (15)$$

where v_t and v_l are the transverse and longitudinal sound velocities in the crystal correspondingly. The long-wave approximation for the acoustic phonons is assumed ($\kappa R_0 \ll 1$). The results for the specific transitions are obtained by the due substitutions of the elements of the matrices $\hat{G}_{\Gamma\gamma}$. They can be found with the use of the irreducible tensor operators technique [2,60–63].

5. Selection rules for one-phonon transitions in pseudo-angular momentum representation

The selection rules for the spin-phonon transitions can be analyzed in terms of the pseudo-angular momentum representation employed for the analysis of the HDVV Hamiltonian and selection rules in EPR transitions reported in V_{15} [8]. It was revealed that the degeneracy doubling (“accidental” degeneracy) in the ground spin-frustrated state $(S_{12})S = (0)1/2, (1)1/2$ is related to the exact orbital degeneracy so that the ground term is the orbital doublet 2E in the trigonal (D_3) symmetry while the excited spin level $S = 3/2$ corresponds to the orbital singlet 4A_2 . This can be symbolically indicated as: $2D^{(1/2)} \Rightarrow {}^2E, 2D^{(3/2)} \Rightarrow {}^2A_2$, where $D^{(S)}$ are the irreducible representations of the rotation group R_3 numerating spin states of the system. It was concluded [61] that the AS exchange acts within the manifold $(S_{12})S = (0)1/2, (1)1/2$ like first order spin-orbital interaction within the 2E term and gives rise to the two doublets in agreement with the Kramers theorem [66].

By applying the symmetry operations of the D_3 point group to the basis functions $|(0)1/2 \pm 1/2\rangle$ and $|(1)1/2 \pm 1/2\rangle$ (that generate permutations of spins in the triangle) one can find that they are related to the x, y basis of the irreducible representation E . Therefore their circular components [67] correspond to the projections $M_L = +1$ and $M_L = -1$ of the pseudo-angular momentum (pseudo-angular momentum representation). We will use a short notation $|M_L, S, M_S\rangle \equiv u_{M_L}(S, M_S)$. The spin functions of the ground manifold can be represented as:

$$\begin{aligned} u_{\pm 1}(1/2, \pm 1/2) &= \mp 1/\sqrt{2}(|(0)1/2, \pm 1/2\rangle \pm i|(1)1/2, \pm 1/2\rangle), \\ u_{\pm 1}(1/2, \mp 1/2) &= \mp 1/\sqrt{2}(|(0)1/2, \mp 1/2\rangle \pm i|(1)1/2, \mp 1/2\rangle). \end{aligned} \quad (16)$$

Using the concept of Russell-Saunders coupling (LS) one can introduce the functions $U_S(M_J)$ belonging to a definite full spin S and projections $M_J = M_L + M_S$ of the full pseudo-angular momentum, so that $U_{1/2}(\pm 3/2) = U_{\pm 1}(1/2, \pm 1/2)$ and $U_{1/2}(\pm 1/2) = U_{\pm 1}(\mp 1/2)$ (LSJ scheme). The orbital singlet 4A_2 corresponds to $M_L = 0$, and the components M_S are labeled as $u_0(3/2, M_S) \equiv U_{3/2}(M_J)$ with $M_S = \pm 1/2$ and $M_S = \pm 3/2$, so that $M_J = \pm 1/2$ and $\pm 3/2$. This labeling is valid for the case of parallel field ($\mathbf{H}||C_3$) that retains the effective axial symmetry of the system. Fig. 3 illustrates the pseudo-angular momentum labels for the Zeeman levels of the system at relatively low field (far enough from the crossing/anti-crossing area) and the selection rules for one-phonon transitions.

The one-phonon transitions have special selection rules that can be illustrated in terms of the pseudo-angular momentum representations providing $\mathbf{H}||C_3$. Although the evaluation of the relaxation times are made (Section 7) in the framework of the general model so far suggested it is worth to underline the specific consequences of different terms in spin-phonon coupling Hamiltonian. Since the isotropic exchange is the main part of exchange interaction, the vibronic coupling related to the modulation of this part of the exchange seems to be dominant. Let us consider different transitions caused by the operator H'_{ev} when magnetic field is parallel to the C_3 axis of the cluster. At low fields the normal component $H_{AS}(\parallel)$ gives rise to a zero field splitting of two $S = 1/2$ levels and there are two allowed transitions which obey the selection rules $\Delta M_L = \pm 2, \Delta M_S = 0, \Delta M_J = \pm 2$ exist in the $S = 1/2$ manifold (solid lines in Fig. 3). When the in-plane part of the AS exchange is taken

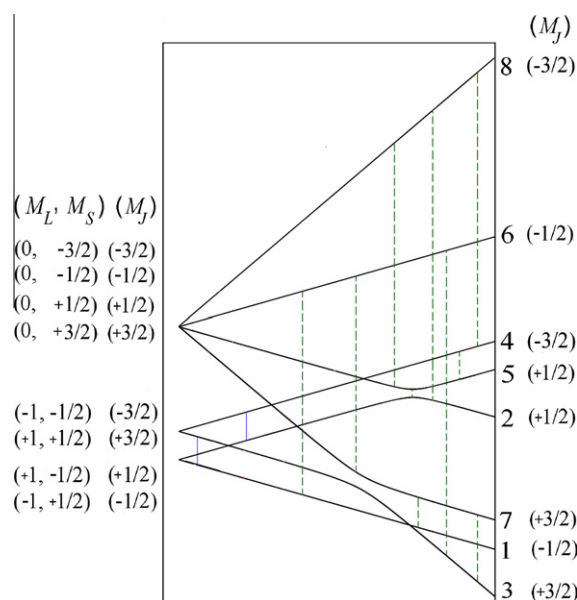


Fig. 3. Zeeman pattern of $V_{15}, \mathbf{H}||C_3$, and transitions caused by the phonon modulation of the isotropic exchange in the presence of the parallel $H_{AS}(\parallel)$ term (solid) or in-plane $H_{AS}(\perp)$ term (dashed) in the Hamiltonian.

into account, it triggers additional transitions since both M_S and M_L are no longer “good” quantum numbers and the only selection rule $\Delta M_J = \pm 2$ remains valid. As one can see there are eight transitions obeying this rule (Fig. 3). It also turns out that the in-plane AS exchange gives rise to the transitions with $\Delta M_J = 0$. These additional transitions are important in the region of level anticrossing where the role of the in-plane AS exchange is most pronounced [5].

In order to find some additional transitions that are forbidden in the framework of the model so far discussed, let us consider transitions caused by the operator $H'_{ev}(\parallel)$ that represents a phonon modulation of the parallel part of AS exchange. The parallel component $H_{AS}(\parallel)$ itself is well pronounced at low fields and in this case there are four transitions between the doublet $S = 1/2$ and quadruplet $S = 3/2$ with the rules $\Delta M_L = \pm 1, \Delta M_S = 0, \Delta M_J = \pm 1$ (Fig. 4).

The numerical calculations based on the full vibronic Hamiltonian will be given in Section 7.

6. Estimation of spin-vibronic coupling parameters

Approximate estimation of spin-vibronic coupling parameters for V_{15} may be done from the available data regarding another

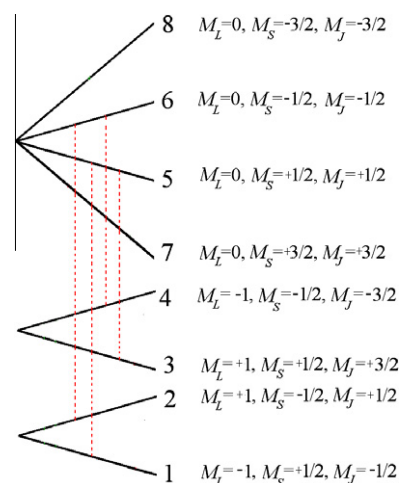


Fig. 4. Transitions caused by the operator $H'_{ev}(\parallel), \mathbf{H}||C_3$.

Table 1

Relaxation times and linewidths for the allowed EPR transitions at 57.9 GHz, 0.5 K, parallel field.

Transition	2	3	12	4	5	1	9
Relaxation time (s)	1.9×10^{-2}	2.4×10^{-3}	2.15×10^{-2}	6.6×10^{-3}	1.1×10^{-2}	1.7×10^{-2}	7.1×10^{-3}
Linewidth (Tesla)	1.9×10^{-9}	1.5×10^{-8}	1.7×10^{-9}	5.5×10^{-9}	4.3×10^{-9}	2.1×10^{-9}	3.4×10^{-9}

Table 2

Relaxation times and linewidths for the allowed EPR transitions at 108 GHz, 0.5 K, parallel field.

Transition	10	2	1	8	3	5
Relaxation time (s)	5.8×10^{-3}	3×10^{-3}	2.5×10^{-2}	1.9×10^{-3}	5.1×10^{-4}	1.6×10^{-3}
Linewidth (Tesla)	3.1×10^{-9}	1.2×10^{-8}	7.3×10^{-10}	1.9×10^{-8}	7.1×10^{-8}	2.2×10^{-8}

compounds. According to Ref. [68] the dependence of J on the interatomic distance R for MnO and MnF₂ is well approximated by the law

$$J = AR^{-3\gamma_m} \approx AR^{-10}, \quad (17)$$

where $\gamma_m \approx 10/3$ is Grüneisen constant and factor A is specific for a given compound. For the V₁₅ cluster one can estimate $A = J_0 R_0^{10}$ (R_0 is the equilibrium metal-metal distances equal to 7 Å in the V^{IV} triangle, $J_0 = 0.85 \text{ cm}^{-1}$ is the equilibrium value of J) and thus the spin-vibronic coupling λ can be found as:

$$\lambda = \sqrt{6} \left(\frac{\partial J_{ij}}{\partial R_{ij}} \right)_0 = -10\sqrt{6}AR_0^{-11} \approx -3 \text{ cm}^{-1}/\text{Å} \quad (18)$$

Assuming that for the components of AS exchange ($\alpha = n, t, l$) the relation

$$\frac{1}{D_{\alpha 0}} \left(\frac{\partial D_{ij\alpha}}{\partial R_{ij}} \right)_0 \cong \frac{1}{J_0} \left(\frac{\partial J_{ij}}{\partial R_{ij}} \right)_0 \quad (19)$$

is valid, one can deduce the following estimation: $\beta_n \approx -0.11 \text{ cm}^{-1}/\text{Å}$, $\beta_{\perp} \approx -0.34 \text{ cm}^{-1}/\text{Å}$.

Alternative estimation of λ is given in ref. [59] where the ratio $(\partial J/\partial R_0)/J$ was found to be in the range $10 - 30 \text{ Å}^{-1}$ for the Ir:ammonium chloroplatinate and ruby with different doping concentration. This estimation gives one order higher values for λ , β_{\perp} , β_n then provided by Eq. (17) but even with this newer estimation spin-vibronic interaction turns out to be very weak.

7. Estimation of the spin-phonon relaxation rates

7.1. The case of weak field

We use the values of the exchange parameters J_0 , D_{\perp} and D_n that are given in Section 2, the spin-phonon coupling parameters $\beta_{\perp} \approx -0.34 \text{ cm}^{-1}/\text{Å}$, $\beta_n \approx -0.11 \text{ cm}^{-1}/\text{Å}$ $R_0 = 7 \text{ Å}$ for the side of the inner triangle in V₁₅, $\rho = 3 \cdot 10^3 \text{ kg/m}^3$ for the density of V₁₅ [69]. Due to the lack of the reliable information regarding the velocities of the sound velocities it is assumed the same values for the transversal and longitudinal velocities $v = 2 \cdot 10^3 \text{ m/s}$. The relaxation times for the low lying levels at 5K are found to be $\tau_{3-1} = \tau_{4-2} = 1.6 \cdot 10^{-3} \text{ s}$ (Fig. 3). These estimations generally agree with the results of Ref. [54] although the estimation presented here gives shorter relaxation times for a definite set of the levels. Of course, the accuracy of these estimations is restricted by the uncertainty of the parameters like sound velocity and spin-vibronic constants. One can see that the modulation of the isotropic exchange gives much faster (two orders of magnitude) transitions than that arising from the modulation of the normal part of AS exchange. But it should be noted that these two mechanisms of spin-phonon transitions obey different selection rules that are expected to give essentially different phonon broadening of EPR lines.

7.2. The case of high field

The numerical estimations based on the full spin Hamiltonian ($H_0 + H_{AS}$) and full spin-phonon Hamiltonian ($H'_{ev} + H''_{ev}$) with the values of parameters defined in Section 6. Fig. 5a and b shows the scheme of EPR transitions (labeled as in Ref. [8]) and their calculated intensities for temperature 0.5K and frequency of 57.9GHz that was used for the low-temperature EPR experiments reported in [70]. The estimated relaxation times and linewidths for the transitions at $\nu = 57.9 \text{ GHz}$ for which the spin-phonon relaxation is allowed by symmetry rules are given in Table 1. Although

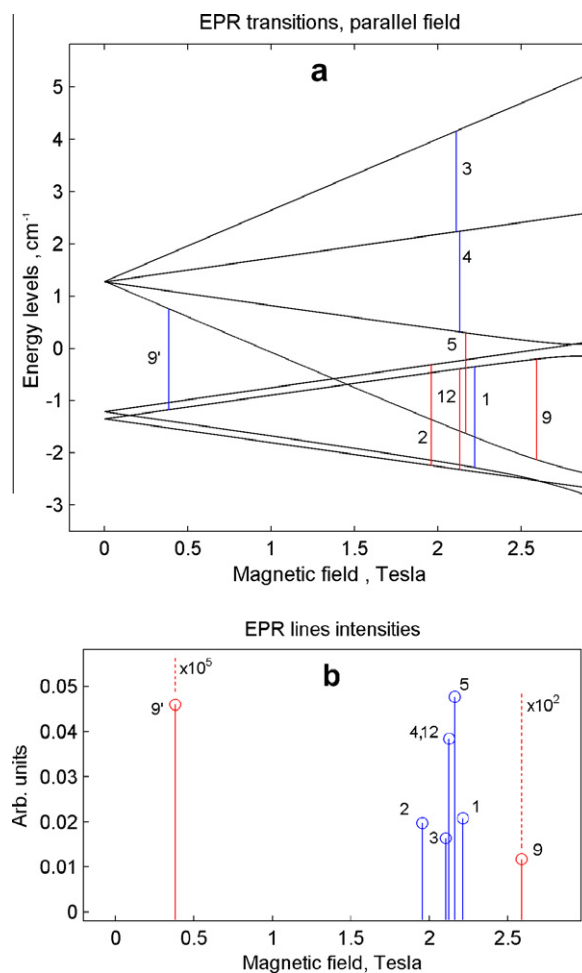


Fig. 5. (a) EPR transitions for the EPR frequency of 57.9 GHz at the temperature of 0.5 K, $\mathbf{H} \parallel \mathbf{C}_3$. Transitions 4 and 12 occur at the same resonant field. (b) Calculated intensities of the lines.

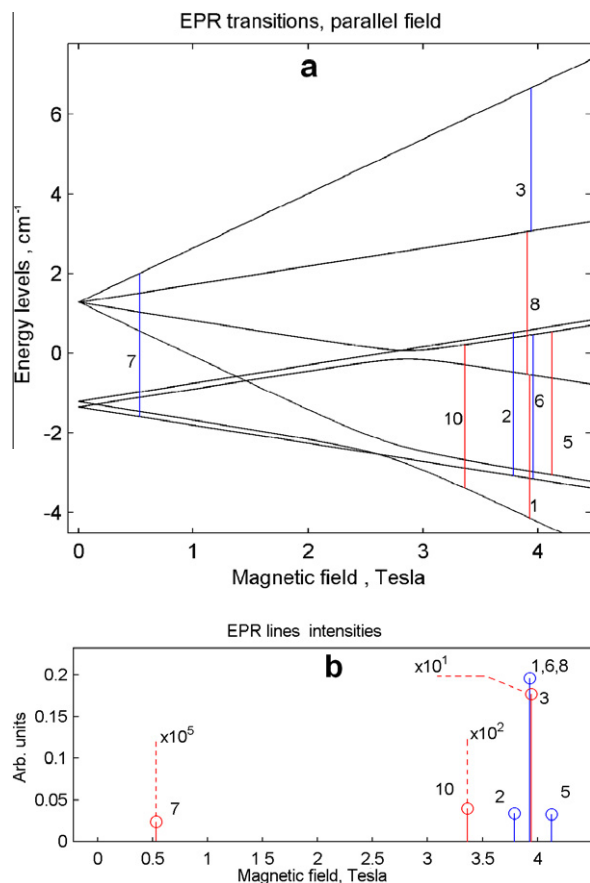


Fig. 6. (a) EPR transitions for 108 GHz at 0.5 T, $H||C_3$. Transitions 1, 6 and 8 occur at the same resonant field but shown with a small artificial shift for the visualization purpose. (b) calculated intensities.

the accuracy in the numerical estimations is restricted by the uncertainty of some parameters (like sound velocity) and approximations so far employed, the interrelations between the relaxation times seem to be reliable for different EPR transitions at different frequencies. Fig. 6 shows the transitions and their comparative intensities at frequency $\nu = 108$ GHz, Table 2 shows relaxation times and linewidths (at the same frequency) for the allowed spin-phonon transitions.

Let us compare the results for different frequencies. Accordingly to the Tables 1 and 2 the relaxation rates decrease with increase of the EPR frequency (due to dependence of the probability as a function of the energy gap) and, consequently, the width of the lines is also increasing. At the frequency 108 GHz these lines are on average four times broader than at 58 GHz. This result is in a reasonable agreement with the broadening observed in Ref. [70], so spin-phonon interaction seems to be a significant factor. It should be noted that the linewidths reported in [70] refer to the absorption line that, constitutes a superposition of the transition lines shown in Figs. 5 and 6.

8. Conclusion

To summarize the results of this article, the following key points are to be mentioned: (1) the model for the spin-phonon coupling for the V_{15} cluster is proposed. The model takes into consideration the modulation of the isotropic and AS exchange interactions within the central V^{IV} triangular spin frustrated layer by the acoustic lattice vibrations (heat reservoir) for which the Debye law of dispersion is assumed; (2) within the pseudo-angular momentum

representation the selection rules for the direct (one-phonon) transitions between Zeeman levels are established and the specific role of different contributions to the spin-phonon coupling is elucidated. An important role of the AS exchange in the selection rule for spin-phonon transitions in spin-frustrated systems is underlined; (3) the numerical results are obtained for different of the field corresponding to the available experimental data on EPR of V_{15} (57.9, 108 GHz). As distinguished from the general estimations, the microscopic approach developed here has allowed to get a detailed information regarding the different direct spin-phonon processes within the Zeeman pattern of the low lying spin excitations in V_{15} . In fact, the relaxation times for one-phonon transitions proved to be specific for the different transitions and ranges of the field. These times for different transitions are estimated as $10^{-2} \div 10^{-4}$ s. The present calculations show that one-phonon processes are less important than the thermal fluctuations of the dipolar interactions between the molecules as a source of decoherence in agreement with the first prediction of coherent states in V_{15} [54].

It should be noted that along with the one-phonon processes another mechanisms of spin-phonon relaxation can play significant (or even dominant) role. These are the two-phonon (Raman type) processes for which the probability can be high due to participation of the two phonons whose frequencies (and consequently phonon densities) are not small as in the case of one-phonon relaxation. Additionally the quadratic (with respect to the atomic displacements) terms of spin-phonon coupling are able to give a significant contribution to the rate of relaxation. The Raman processes in V_{15} are expected to be especially important due to the high density of the excited spin states (dimension of the Hilbert space is 10^{15}) virtually involved in the second order processes. The Orbach type relaxation should also be taken in consideration with due account for the excited spin states and their detailed Zeeman structure. We plan to extend the presented model in future paying special attention to the problem of decoherence in molecular magnets.

Acknowledgment

This work is done under the auspices of the Israel Science Foundation (ISF) whose financial support is gratefully acknowledged (Grant No. 168/09).

Appendix I

The operators $\hat{V}_{T\gamma}$ in terms of the scalar products of spin operators:

$$\hat{V}_A = \sqrt{\frac{2}{3}}(\mathbf{S}_1\mathbf{S}_2 + \mathbf{S}_2\mathbf{S}_3 + \mathbf{S}_3\mathbf{S}_1),$$

$$\hat{V}_X = \frac{1}{\sqrt{6}}(\mathbf{S}_2\mathbf{S}_3 + \mathbf{S}_3\mathbf{S}_1 - 2\mathbf{S}_1\mathbf{S}_2),$$

$$\hat{V}_Y = \frac{1}{\sqrt{2}}(\mathbf{S}_2\mathbf{S}_3 - \mathbf{S}_3\mathbf{S}_1).$$

The operators $\hat{W}_{T\gamma}$ in terms of the vector products of spin operators:

$$\hat{W}_A = \mathbf{e}_{12}[\mathbf{S}_1 \times \mathbf{S}_2] + \mathbf{e}_{23}[\mathbf{S}_2 \times \mathbf{S}_3] + \mathbf{e}_{31}[\mathbf{S}_3 \times \mathbf{S}_1],$$

$$\hat{W}_X = \frac{1}{\sqrt{2}}(\mathbf{e}_{12}[\mathbf{S}_1 \times \mathbf{S}_2] + \mathbf{e}_{23}[\mathbf{S}_2 \times \mathbf{S}_3] - 2\mathbf{e}_{31}[\mathbf{S}_3 \times \mathbf{S}_1]),$$

$$\hat{W}_Y = \frac{\sqrt{6}}{2}(\mathbf{e}_{23}[\mathbf{S}_2 \times \mathbf{S}_3] - \mathbf{e}_{31}[\mathbf{S}_3 \times \mathbf{S}_1]).$$

where \mathbf{e}_{ij} denotes the unit vector in direction of the vector β_{ij} .

Appendix II

The Van Vleck coefficients $a_{\kappa}(\Gamma\gamma)$ for the equilateral triangular unit are given by the following equations [59]:

$$a_{\kappa}(A_1) = (1/2)(\kappa R_0)(l'l' + m'm'),$$

$$a_{\kappa}(E_X) = -(1/2)(l'l' - m'm'),$$

$$a_{\kappa}(E_Y) = -(1/2)(\kappa R_0)(l'm' - m'l')$$

where R_0 is the side of a triangle, l' , m' and n' are the direction cosines of the wave-vector in the coordinate system defined in Fig. 2, and l , m , n are direction cosines of polarization vector. In the long-wave Debye approximation $\kappa = \omega/v_v$. In this approximation the coefficients $|a_{\kappa}(\Gamma\gamma)|^2$ can be averaged over all propagation and polarization directions. The result is the following:

$$\langle a_t^2(A_1) \rangle = \frac{2}{15} \frac{\omega^2 R_0^2}{v_t^2}, \quad \langle a_t^2(E_X) \rangle = \frac{1}{15} \frac{\omega^2 R_0^2}{v_t^2}, \quad \langle a_t^2(E_Y) \rangle = \frac{1}{15} \frac{\omega^2 R_0^2}{v_t^2}$$

$$\langle a_t^2(A_1) \rangle = \frac{\omega^2 R_0^2}{60 v_t^2}, \quad \langle a_t^2(E_X) \rangle = \frac{\omega^2 R_0^2}{20 v_t^2}, \quad \langle a_t^2(E_Y) \rangle = \frac{\omega^2 R_0^2}{20 v_t^2}$$

References

- [1] S. Bertaina, S. Gambarelli, T. Mitra, B. Tsukerblat, A. Müller, B. Barbara, *Nature* 453 (2008) 20.
- [2] D. Gatteschi, R. Sessoli, J. Villain, *Molecular Nanomagnets*, Oxford University Press, Oxford, 2006.
- [3] A.L. Barra, D. Gatteschi, B.S. Tsukerblat, J. Döring, A. Müller, L.-C. Brunel, *Inorg. Chem.* 31 (1992) 5132.
- [4] D. Gatteschi, B. Tsukerblat, A.L. Barra, L.C. Brunel, A. Müller, J. Döring, *Inorg. Chem.* 32 (1993) 2114.
- [5] B. Tsukerblat, A. Tarantul, A. Müller, *Phys. Lett. A* 353 (2006) 48.
- [6] A. Müller, S. Talismanov, P. Kögerler, H. Bögge, M. Schmidtman, B. Tsukerblat 16 (2005) 391.
- [7] A. Tarantul, B. Tsukerblat, A. Müller, in: *Nanometer-Scale Molecular Cluster V₁₅: EPR and Adiabatic Magnetization*, fourth International Conference on Mathematical Modeling and Computer Simulation of Materials Technologies, Ariel, Israel, 2006, p 103.
- [8] B. Tsukerblat, A. Tarantul, A. Müller, *J. Chem. Phys.* 125 (2006) 0547141.
- [9] B. Tsukerblat, A. Tarantul, A. Müller, *Chem. J. Moldova* 2 (1) (2007) 17.
- [10] A. Müller, M.T. Pope, Ana M. Todea, H. Bögge, Joris van Slageren, M. Dressel, P. Gouzerh, R. Thouvenot, B. Tsukerblat, A. Bell, *Angew. Chem.* 119 (2007) 4561.
- [11] A. Tarantul, B. Tsukerblat, A. Müller, *Solid State Sci.* 10 (2008) 1814.
- [12] A. Tarantul, B. Tsukerblat, A. Müller, *J. Mol. Struct.* 890 (2008) 170.
- [13] P. Kögerler, B. Tsukerblat, A. Müller, *Dalton Trans.* 39 (2010) 21.
- [14] A. Müller, J. Döring, *Angew. Chem., Int. Ed.* 27 (1988) 1719.
- [15] D. Gatteschi, L. Pardi, A.L. Barra, A. Müller, J. Döring, *Nature* 354 (1991) 465.
- [16] A.L. Barra, D. Gatteschi, L. Pardi, A. Müller, J. Döring, *J. Am. Chem. Soc.* 114 (1992) 8509.
- [17] D. Gatteschi, L. Pardi, A.L. Barra, A. Müller, *Mol. Eng.* 3 (1993) 157.
- [18] B. Barbara, *J. Mol. Struct.* 656 (2003) 135.
- [19] I. Chiorescu, W. Wernsdorfer, A. Müller, H. Bögge, B. Barbara, *J. Magn. Magn. Mater.* 221 (2000) 103.
- [20] I. Chiorescu, W. Wernsdorfer, A. Müller, H. Bögge, *Phys. Rev. Lett.* 84 (2000) 3454.
- [21] S. Miyashita, *J. Phys. Soc. Jpn.* 65 (1996) 2734.
- [22] H. Nojiri, T. Taniguchi, Y. Ajiro, A. Müller, B. Barbara, *Physica B* 216 (2004) 346.
- [23] S. Miyashita, *J. Phys. Soc. Jpn* 64 (1995) 3207.
- [24] V.V. Platonov, O.M. Tatsenko, V.I. Plis, A.K. Zvezdin, B. Barbara, *Phys. Solid State* 44 (2002) 2010.
- [25] V.V. Kostyuchenko, A.I. Popov, *J. Exp. Theor. Phys.* 107 (4) (2008) 595.
- [26] C. Raghun, I. Rudra, D. Sen, S. Ramasesha, *Phys. Rev. B* 68 (2003) 029902.
- [27] S. Miyashita, H. De Raedt, K. Michielsen, *Prog. Theor. Phys.* 110 (2003) 889.
- [28] H. De Raedt, S. Miyashita, K. Michielsen, M. Machida, *Phys. Rev. B* 70 (2004) 064401.
- [29] H. De Raedt, S. Miyashita, K. Michielsen arXiv: cond-mat/0306275v1, (2003).
- [30] H. De Raedt, S. Miyashita, K. Michielsen, *Phys. Status Solidi B* 241 (2004) 1180.
- [31] N.P. Konstantinidis, D. Coffey, *Phys. Rev. B* 66 (2002) 174426.
- [32] M. Machida, S. Miyashita, *Physica E* 29 (2005) 538.
- [33] J. Kortus, M.R. Pederson, C.S. Hellberg, S.N. Khanna, *Eur. Phys. J. D* 16 (2001) 177.
- [34] J. Kortus, C.S. Hellberg, M.R. Pederson, *Phys. Rev. Lett.* 86 (2001) 3400.
- [35] D.W. Boukhvalov, E.Z. Kurmaev, A. Moiwes, D.A. Zatsepin, V.M. Cherkashenko, S.N. Nemnonov, L.D. Finkelstein, Yu.M. Yarmoshenko, M. Neumann, V.V. Dobrovitski, M.I. Katsnelson, A.I. Lichtenstein, B.N. Harmon, P. Kögerler, *Phys. Rev. B* 67 (2003) 134408.
- [36] D.W. Boukhvalov, V.V. Dobrovitski, M.I. Katsnelson, A.I. Lichtenstein, B.N. Harmon, P. Kögerler, *Phys. Rev. B* 70 (2004) 054417.
- [37] A. Barbour, R.D. Luttrell, J. Choi, J.L. Musfeldt, D. Zipse, N.S. Dalal, D.W. Boukhvalov, V.V. Dobrovitski, M.I. Katsnelson, A.I. Lichtenstein, B.N. Harmon, P. Kögerler, *Phys. Rev. B* 74 (2006) 014411.
- [38] G. Chaboussant, R. Basler, A. Sieber, S.T. Ochsenbein, A. Desmedt, R.E. Lechner, M.T.F. Telling, P. Kögerler, A. Müller, H.-U. Güdel, *Europhys. Lett.* 59 (2) (2002) 291.
- [39] G. Chaboussant, S.T. Ochsenbein, A. Sieber, H.-U. Güdel, H. Mutka, A. Müller, B. Barbara, *Europhys. Lett.* 66 (3) (2004) 423.
- [40] B. Tsukerblat, A. Tarantul, *The nanoscopic V₁₅ cluster: a unique magnetic polyoxometalate*, in: R.E.P. Winpenny (Ed.), *Molecular Cluster Magnets*, World Scientific Publishers, Singapore, 2010 (in press).
- [41] R.E.P. Winpenny, *Angew. Chem., Int. Ed.* 47 (2008) 2.
- [42] D. Loss, M.N. Leuenberger, *Nature* 410 (2001) 789.
- [43] S.B. Braun-Sand, O. Wiest, *J. Phys. Chem. A* 107 (2003) 285.
- [44] F. Troiani, A. Ghirri, M. Affronte, S. Carretta, P. Santini, G. Amoretti, S. Piligkos, G. Timco, R.E.P. Winpenny, *Phys. Rev. Lett.* 94 (2005) 207208.
- [45] M. Affronte, F. Troiani, A. Ghirri, S. Carretta, P. Santini, V. Corradini, R. Schuecker, C. Muryn, G. Timco, R.E.P. Winpenny, *Dalton Trans.* (2006) 2810.
- [46] A. Ardavan, O. Rival, J.J.L. Morton, S. Blundell, A.M. Tyryshkin, G.A. Timco, R.E.P. Winpenny, *Phys. Rev. Lett.* 98 (2007) 057201.
- [47] M. Affronte, F. Troiani, A. Ghirri, A. Candini, M. Evangelisti, V. Corradini, S. Carretta, P. Santini, G. Amoretti, F. Tuna, G. Timco, R.E.P. Winpenny, *J. Phys. D: Appl. Phys.* 40 (2007) 2999.
- [48] S. Carretta, P. Santini, G. Amoretti, F. Troiani, M. Affronte, *Phys. Rev. B* 76 (2007) 024408.
- [49] D. Stepanenko, M. Trif, D. Loss, *Inorg. Chim. Acta* 361 (2008) 3740.
- [50] A. Morello, P.C.E. Stamp, I.S. Tupitsyn, *Phys. Rev. Lett.* 97 (2006) 207206.
- [51] J. Lehmann, A. Gaita-Arino, E. Coronado, D. Loss, *Nat. Nanotechnol.* 2 (2007) 312.
- [52] G. Mitrikas, Y. Sanakis, C.P. Raptopoulou, G. Kordas, G. Papavassiliou, *Phys. Chem. Chem. Phys.* 10 (2008) 743.
- [53] C. Schlegel, J. van Slageren, M. Manoli, E.K. Brechin, M. Dressel, *Phys. Rev. Lett.* 101 (2008) 147203.
- [54] V.V. Dobrovitski, M.I. Katsnelson, B.N. Harmon, *Phys. Rev. Lett.* 84 (2000) 3458.
- [55] I.E. Dzyaloshinsky, *Zh. Exp. Teor. Fiz.* 32 (1957) 1547.
- [56] T. Moriya, *Phys. Rev. B* 120 (1960) 91.
- [57] A. Tarantul, B. Tsukerblat, A. Müller, *Inorg. Chem.* 46 (1) (2007) 161.
- [58] B. Tsukerblat, A. Tarantul, A. Müller, *J. Mol. Struct.* 838 (2007) 124.
- [59] A. Tarantul, B. Tsukerblat, A. Müller, *Chem. Phys. Lett.* 428 (2006) 361.
- [60] C.A. Bates, R.F. Jasper, *J. Phys. Chem. C* 4 (1971) 2341.
- [61] B.S. Tsukerblat, M.I. Belinskii, *Magnetochemistry and Radiospectroscopy of Exchange Clusters (Rus)*, Stiintsa, Kishinev, 1983.
- [62] B.S. Tsukerblat, M.I. Belinskii, V.E. Fainzilberg, *Magnetochemistry and Spectroscopy of Transition Metal Exchange Clusters*, in: *Soviet Sci. Rev. B.M. (Eds.)*, Harwood Acad. Pub. New York, 1987, vol. 9, p. 337.
- [63] D.A. Varshalovich, A.N. Moskalev, V.K. Khersonskii, *Quantum Theory of Angular Momentum*, World Scientific, Singapore, 1988.
- [64] A. Bencini, D. Gatteschi, *Electron Paramagnetic Resonance of Exchange Coupled Systems*, Springer, Berlin, 1990.
- [65] R. Schnalle, J. Schnack, *Int. Rev. Phys. Chem.* 29 (2010) 403.
- [66] J.H. Van Vleck, *Phys. Rev.* 57 (1940) 426.
- [67] B.S. Tsukerblat, *Group Theory in Chemistry and Spectroscopy. A Simple Guide to Advanced Usage*, Dover Pub, Mineola, NY, 2006.
- [68] R.M. White, T.H. Geballe, *Solid State Physics Advances in Research: Long Range Order in Solids (Solid state physics: Supplement)*, Academic Press, 1979.
- [69] A. Müller, J. Döring, Private Communication.
- [70] T. Sakon, K. Koyama, M. Motokawa, Y. Ajiro, A. Müller, B. Barbara, *Physica B* 206 (2004) 346.